Optimization of Disposal Method and Scenario to Reduce High Level Waste Volume and Repository Footprint for HTGR

Yuji Fukaya[1]*, Minoru Goto[1], Hirofumi Ohashi[1], Tetsuo Nishihara[1], Yasuhiro Tsubata[2], and Tatsuro Matsumura[2]

[1]HTGR Hydrogen and Heat Application Research Center

[2]Nuclear Science and Engineering Center

Japan Atomic Energy Agency (JAEA)

4002 Narita-cho, Oarai-machi, Higashiibaraki-gun,Ibaraki 311-1393, Japan

*E-mail: fukaya.yuji@jaea.go.jp

Phone: +81-29-267-1919-3837

Fax: +81-29-266-7703

Total number of pages: 58

Total number of Tables: 15

Total number of Figures: 10

Abstract

To reduce volume of High Level Waste (HLW) and the footprint in the geological repository of a High Temperature Gas-cooled Reactor (HTGR), this study optimizes the disposal method and scenario of the HLW.

By virtue of high burn-up, high thermal efficiency and pin-in-block type fuel, the HTGR more effectively reduces the HLW volume and its footprint than those of Light Water Reactor (LWR) in our previous study. In this study, the disposal method and scenario are optimized. To optimize the disposal method, the geological repository layout is the horizontal emplacement based on the KBS-3H concept, rather than the vertical emplacement based on the KBS-3V concept adopted in our previous study.

In comparison with the earlier study, the horizontal emplacement reduced the repository footprint in direct disposal by 20 % in the same scenario. By extending the cooling time by 40 years before disposal, the footprint was reduced by 50 %. In disposal with reprocessing, extending cooling time by 1.5 years between discharge and reprocessing reduced the number of canister generated by 20 %. Extending the cooling time by 40 years pre-disposal reduced the footprint per unit of electricity generation by 80 %.

Moreover, by employing four-group partitioning technology without transmutation, the footprint can be reduced by 90 % with a cooling time of 150 years.

KEYWORDS: HLW, footprint, high burn-up, HTGR, GTHTR300, four-group partitioning

Highlight

- Canister numbers and its footprint of disposal processes were evaluated in an HTGR.
- Waste reduction was optimized by horizontal emplacement and proper disposal scenario.
- Footprint was reduced by 50 % in direct disposal and 80 % in disposal with reprocessing.
- Four-group partitioning technology reduced the footprint by 90% from reference.

1. Introduction

High Temperature Gas-cooled Reactors (HTGRs) have attracted a huge attention from a safety point of view (Ohashi, et al. 2011), especially from the Fukushima Daiichi nuclear power plant disaster in Japan in 2011. The environmental burden of radioactive waste is the most important consideration in Nuclear Power Generation (NPG). After the disaster, the significance of nuclear technology was frequently questioned and discussed. In this context, the number of High Level radioactive Waste (HLW) packages and the footprint in a geological repository for HTGR were evaluated in the previous study (Fukaya, et al. 2016).

The Gas Turbine High Temperature Reactor (GTHTR300) (Yan, et al. 2003) is an annular-core type HTGR that generates 600 MW thermal power from pin-in-block type fuel. The major specifications of the GTHTR300 (Nakata, et al. 2003) are listed in Table 1. The burn-up is approximately 120 GWd/t, approximately triple that of Light Water Reactor (LWR) with a burn-up of 45 GWd/t. Moreover the thermal efficiency is 30 % higher in an HTGR than that in a LWR (45.6% versus 34.5 %). Consequently,

HTGR generate less HLW LWRs. The previous study proposed an effective waste-loading method that exploits pin-in-block type fuel. In direct disposal and disposal with reprocessing, this method reduces the number of canisters and the footprint per electricity generation of the HTGR by 60 % and 30 % respectively, compared with those of PWR case.

Previous study has adopted vertical emplacement based on the KBS-3V concept (SKB, 2010) named after its proposer, Svensk Kärnbränslehantering AB (SKB), which is the most achievable one. As HTGR waste generates less heat than LWR waste, the geological repository footprint of vertical emplacement is determined by structural limitations, which ensure the structural integrity of the repository. Meanwhile, in horizontal emplacement based on the KBS-3H concept (SKB, 2010), only the drift intervals must be structurally limited. The small drift diameter reduces the structural limitations, thus reducing the repository footprint. The waste package pitches are unrelated to the repository integrity, and are determined only by the dimensions of the engineering barrier. Owing to its lower footprint, horizontal displacement is dominated by thermal limitation, which confers a buffer functionality. Therefore, the disposal scenario should be reconsidered to reduce the footprint with the decaying heat generation. Moreover, the number of waste packages generated in disposal with reprocessing can be reduced by extending the cooling time between discharge and reprocessing.

Partitioning & Transmutation (P&T) is another popular method that reduces the volume and footprint of HLW. Therefore, this study also considers partitioning technology, which has been already demonstrated.

The present study seeks the optimal disposal method and scenario that could

reduce the volume and footprint of HTGR-generated HLW as an introductory option, without requiring innovative technology. The disposal method is optimized by changing the disposal layout of horizontal emplacement and the waste pitches. The disposal scenario was optimized by changing the duration between the spent fuel discharge, reprocessing and disposal. To optimize the process, the cooling time before disposal is limited to within 100 years (to within 150 years in the partitioning case). Section 2 summarizes the major results and calculation conditions of the previous study, and Section 3 describes the optimal disposal scenario and calculation method of the present study. The repository layout of each disposal scenario is designed in Section 4. The waste reduction effect of the partitioning technology is investigated in Section 5. Finally, the acceptance of the proposed disposal scenario and the HLW volume and footprint reduction of the scenario are described in Section 6.

2. Evaluation Conditions, Methods and Reference Case in the Previous Study

2.1 Scenario, Geological Repository Design, and Safety Requirement

In the previous study, the reduction effect on HLW volume and its footprint were evaluated and compared with those of LWR. The scenario, repository design, and specifications for the disposal of HLW generated from the LWR fuel cycle are given in the Japan Atomic Energy Commission (JAEC) report (JAEC, 2004). According to this plan, the Spent Fuels (SFs) are reprocessed 4 years after discharge, and the vitrified wastes are disposed of 50 years after reprocessing (54 years after discharge). Directly disposed SFs are disposed of 54 years after discharge to match the disposal-with-reprocessing plan.

The most achievable configuration, namely, vertical emplacement based on the KBS-3V concept (SKB, 2010) described in Section 1, was selected as the reference case. The repository design depends on two parameters: the tunnel interval and the waste package pitch. These parameters are limited by the safety requirement of structural integrity and maintenance of the buffer function. The limitations imposed by structural integrity were evaluated by structural analysis (JAEC, 2004), and they were taken into the previous study. In maintaining the buffer function, the main problem is the maximum temperature in the bentonite buffer. When the temperature exceeds 100 °C, the high temperature changes its property and loses its ability to delay nuclide migration. To allow for uncertainties, the target upper temperature is set to 90 °C (JAEC, 2004). The maximum temperature of the bentonite for the HTGR case was evaluated by time-dependent thermal conductivity calculations performed in ANSYS code (ANSYS Inc., 2013), which solves the thermal equation by the finite element method with an implicit time integral technique.

In addition, the waste must never reach criticality in the repository forever. In direct disposal, the waste package includes residual ^{235}U, and generated ^{239}Pu and ^{241}Pu. Criticality safety is also confirmed in MVP calculations (Nagaya et al. 2006). MVP is a neutron transport calculation code based on the Monte Carlo method, and the calculations use evaluated nuclear data of JENDL-4.0 (Shibata et al. 2011). MVP code is suitable for HTGR calculation because it applies a statistical geometry model that handles the double heterogeneity effect, the self-shielding effect caused by the complicated geometry of Coated Particle Fuel (CPF) (Murata et al. 1997).

2.2 Burn-up Calculation and Characteristics of Heat Generation

The fuel burn-up composition and decay heat were evaluated in ORIGEN (Croff, 1983) code. However, ORIGEN code cannot evaluate the neutron spectrum in a core and uses a single energy group cross section libraries. Libraries for the major reactors have been already developed. The Japan Nuclear Data Committee (JNDC) has developed ORIGEN library of ORLIBJ40 (Okumura et al. 2012) based on evaluated nuclear data of JENDL-4.0. ORLIBJ40 includes libraries for LWRs and Fast Breeder Reactors (FBRs). In the previous study, the PWR47J40 library in ORLIBJ40 was used for Pressurized Water Reactor (PWR) calculations, and libraries for HTGR (which did not previously exist) with the nuclear characteristics of GTHTR300 were evaluated by MVP code using the evaluated nuclear data of JENDL-4.0, JEFF-3.1.2 (Koning et al. 2011a), JENDL/A-96 (Nakajima, 1991), JEFF-3.1/A (Koning et al. 2006) and TENDL-2011 (Koning et al. 2011b).

The burn-up compositions and decay heats of the PWR and HTGR were calculated under the conditions listed in Table 2. The decay heat per burn-up curves are shown in Fig. 1. The decay heats of Fission Products (FPs) from HTGR and LWR coincide. The actinoid decay heats are approximately 20 % smaller in the HTGR than in the PWR because HTGR generates fewer TRans Uranium (TRU) nuclides. Apart from neptunium, the TRU nuclides are converted from ^{238}U. The generated weight per burn-up of HTGR is approximately half that of PWR because (relative to the PWR) the neutron flux level in the HTGR is halved while the ^{235}U fission cross sections are double. These properties are conferred by the well moderated spectrum. In an HLW with reprocessing, 0.442 % of the uranium and 0.548 % of the plutonium are added in vitrified form. The other actinoid elements are assumed to be vitrified at 100.0%. (JNC, 2000a)

The FP decay heats decay more rapidly than the actinoid decay heats. In direct

disposal in the HTGR, the decay heat of the FPs become lower than that of the actinoids in 70 years after discharge. In disposal with reprocessing, the decay heats of the FPs dominate until 150 years post-discharge. The decay heat is expected to be effectively reduced by extending the cooling time during time of dominant FP decay heat.

Tables 2, 3 and Fig.1

2.3 Number of Waste Packages and Footprint with Vertical Emplacement

The number of waste packages and its footprint evaluated in the previous study is listed in Table 3, which lists the major specifications of the reactor and fuel. Owing to the higher burn-up, higher thermal efficiency, and effective waste-loading method proposed in this study, for direct disposal, HTGR generates fewer canisters (1.20 canisters/TWeh) than the PWR (2.92 and 1.46 canisters/TWeh, for 2 and 4 assemblies per canister case, respectively). The waste production is 60% and 20 % lower than that of the 2 and 4 assemblies per canister case of PWR, respectively. The footprint per unit of electricity generation (244.0 m^2/TWeh) by the HTGR is 60 % and 50 % lower than that of the 2 assemblies per canister case (560.1 m^2/TWeh) and 4 assemblies per canister case (466.8 m^2/TWeh) in the PWR, respectively. Owing to the low decay heat with less TRU generation, the relatively low footprint per electricity generation in HTGR is also contributed by the small footprint per canister. The footprint per canister in the HTGR (204.0 m^2/canister) almost equals that of the 2 assemblies per canister case of PWR (192.0 m^2/canister) but is 40 % lower than that of the 4 assemblies per canister (320.0 m^2/canister). Direct disposal in the HTGR maintains sufficient subcritical conditions of the repository. However, in the PWR, 4 assemblies per canister case reaches unless the poison effects of FPs are included. Therefore, to ensure safe subcriticality of the LWR, 2 assemblies per canister case should be the representative

case.

In disposal with reprocessing, the HTGR reduces the generated number of canisters and the repository footprint per electricity generation by 30 % (relative to LWR), reflecting the 30 % increase in thermal efficiency.

When fabricating the vitrified form, the number of canister generated in disposal with reprocessing is determined by the heat generation limitation. Meanwhile, in both direct disposal and disposal with reprocessing, the repository footprints per canister are determined by the structural limitation. The number of vitrified waste generated and the footprint can be reduced by configuring the horizontal emplacement and optimizing the disposal scenario as described in Section 1.

3. Optimization and Evaluation Method

3.1 Optimization of Disposal Scenario

In the reference scenario, the SFs are reprocessed 4 years after discharge, and the vitrified wastes are disposed of 50 years after reprocessing (54 years after discharge). In direct disposal, the SFs are disposed of after 54 years to match the reprocessing plan (see Section 2.2). In direct disposal, the only option is extending the cooling time before disposal to reduce the repository footprint. On the contrary, the number of vitrified waste (which is limited by heat generation as described in Section 2.3) can be reduced by setting the cooling time between discharge and reprocessing.

Table 4 lists the specifications and limitations (JNC, 2000a, and Inagaki et al. 2009) of the vitrified waste generated by HTGR. In this study, the specifications of the waste package were determined not to exceed these limitations, but the actual waste

fabrication must allow a safety margin. The number of waste packages is determined by the limitation of allowed heat generation at vitrification. To prevent phase transmutations such as crystallization and liquid-liquid phase separations at elevated temperatures caused by the decay heat, the temperature of the stored waste must remain below 500°C; this limits the waste package generation to 2.3 kW/canister. From the viewpoint of radioactive nuclide confinement, the content of waste oxides, FP oxide, and actinide oxide should not exceed 15 wt%. Limiting the MoO_3 content to 1.5 wt% prevents the formation of Mo-rich phase (the so-called yellow phase), and it also preserves the chemical durability of the vitrified form. Meanwhile, if the content of Platinum Group Metals (PGMs) exceeds 1.25 wt%, the lifetime of Liquid Fed Ceramic Melter (LFCM) is reduced. PGMs such as Ru, Rh, and Pd are insoluble in the borosilicate waste glass matrix and tend to form separate phases of RuO_2 and Pd-Rh-Te alloys in the molten glass. When these phases accumulate at the melter bottom, they form electrical short circuits that dissipate the power and corrodes the electrodes, thereby shortening the melter lifetime. The heat generation can be limited by setting the cooling time before vitrification although this solution increases the waste oxide content. However, to satisfy the other limitations, the specification of the vitrified form and melter must be improved, and/or an additional separation process must be introduced into the reprocessing that prevents the contents from accumulating beyond the limitations. In general, the dominant secondary limitation is due to the MoO_3 content. The initial heavy metal inventory of SF per canister at the limit of the MoO_3 content is listed in Table 5. The initial heavy metal inventory of SF per canister is 30 % higher than that in the reference case. Without a scenario change, the heat generation at vitrification is 3.0 kW/canister, which is above the limitation of 2.3 kW/canister. To

reduce the decay heat to 2.2 kW/canister, the cooling time between the discharge and reprocessing should be extended by 1.5 years. For such a short cooling time, of 1.5 years is so short that there is no need to change the term from discharge to disposal.

Tables 4 and 5

3.2 Optimization Method for Repository Design

The repository design is determined by the bentonite buffer temperature as described in Section 2.1. The layout must satisfy the structural limitations. The thermal calculations were performed in ANSYS code (ANSYS, Inc. 2013), and the model was developed through the research of JAEC (JAEC, 2004) as shown in Fig. 2. The waste packages are located 500 m underground. The host rock is assumed as soft rock. The drift interval in the horizontal emplacement is structurally restricted to 6.86 m in direct disposal (JAEC, 2004) and 5.55 m in disposal with reprocessing (JNC, 2000a). The lengths of the minimum waste package pitches, determined by the dimensions of the engineering barrier, are 6.08 m (JAEC, 2004) and 3.13 m (JNC, 2000a), in direct disposal and disposal with reprocessing, respectively. To validate the thermal calculation method and model, this study presents the thermal calculation results in direct disposal of PWR SFs. The decay heat was evaluated in ORIGEN code using the PWR47J40 library in ORLIBJ40 as described in Section 2.2. The canister contains 4 fuel assemblies. With the canister pitch and drift interval set to 10.0 m and 31.0 m, respectively, the maximum bentonite temperature was determined as 90.8 °C. The close agreement with the maximum temperature of 90 °C reported by JAEC (JAEC, 2004) validate the analysis.

Fig.2

Moreover, direct disposal should maintain subcriticality in the repository. The subcriticality condition was evaluated by MVP code in JENDL-4.0 as described in

Section 2.1. The waste package of the HTGR was fabricated by the effective waste-loading method proposed in our previous study. In this concept, the HTGR spent fuel is loaded into the same canister as PWR. The fuel rods of pin-in-block type fuels can be withdrawn from the fuel block and can be inserted into the canister as shown in Fig. 3. This treatment significantly reduces the volume of the HLW can be achieved. In the criticality calculation, it is assumed that the carbon steel canister will be corroded and flown out. Subsequently, as it occurs in the LWR model (JAEC, 2004), the region will be filled with groundwater (also shown in Fig. 3). This model retains the fuel rods, which are constructed from graphite and the Coated Fuel Particles (CFPs) play a fuel-containment role. When developing this model in the previous study, we considered the high durability of graphite material, the failure mechanism of CFPs, and the dissolution and outflow mechanism of the fuel material. The geometric model of the repository is shown in Fig. 4. The lattice arrangement, which influences the neutronic interactions, is realized by imposing reflective boundary conditions. The buffer comprises montmorillonite (70 wt%) and silica sand (30 wt%) with a moisture content of 7 %. The soft rock is represented by sandstone with a moisture content of 30 %. To obtain a conservative result, the temperature of the waste and repository is assumed to be 30 ℃ (the underground temperature at a depth of 500 m). The actual temperature and criticality are raised and lowered, respectively, by the negative reactivity of the Doppler effect induced in the large amount of ^{238}U. The representative multiplication factor is the upper side of three standard deviations, whose statistical distribution was determined using MVP calculation based on the Monte Carlo method.

Figs.3 and 4

4. Optimization Result of Disposal Method and Scenario

4.1 Repository Footprint for Direct Disposal

The repository footprints determined by the thermal calculations are listed in Table 6. The cooling time from discharge to disposal is extended by up to 40 years to reduce the repository footprint. Figure 5 plots the graph for repository footprint versus the extended cooling time. The footprint is significantly reduced by extending the cooling time by 20 years because the heat generated by the FPs dominates in this period (see Section 2.2). More than 40 years, the reduction effect of cooling time is weakened because the decay heat from the FPs has decayed to a negligible amount, and most of the heat is now generated by actinoids. Figure 6 shows the change in the maximum bentonite temperature after disposal. The maximum bentonite temperature appears after the temperature increase of host rock and its saturation. Extending the cooling time delays the time of maximum temperature, hence, reduces the amount of decay heat at that time. This effect further reduces the repository footprint.

Criticality safety is also confirmed in the strictest case that it minimizes repository footprint (see Fig.7). At 54–100 years post-discharge, the criticalities are lowered by the decay of ^{241}Pu but are later increased by the decays of ^{238}Pu, ^{240}Pu, and ^{241}Am. The criticality first peaks are observed at approximately 80,000 years because ^{239}Pu decays with a half-life of 24,100 years. Later, the criticality recovers as the ^{242}Pu decays. The second peaks appear at approximately 10 million years. Ultimately, the criticality declines as the residual ^{235}U (with a half-life of 703.5 million years) decays. With a multiplication factor below 0.8, sufficient subcriticality is confirmed at all times. As described in Section 3.2, the poison effect of FPs is considerable because of the high confinement function of CFPs and high durability of their structural material made of graphite. However, subcriticality is ensured despite excluding the poison effect of FPs.

To guard against particular accident scenarios, the criticality safety could be tightened by employing B_4C-C composite, which is employed as burnable poison in HTGR, and expected high durability for ground water as same as other graphite materials, can be employed as fuel rods binder and neutron absorber.

Table 6 and Figs.5,6, and 7

4.2 Number of Waste Packages and Footprint in Disposal with Reprocessing

In the increased-waste scenario of disposal with reprocessing, the initial heavy metal inventory of SF per canister is 30 % higher than that in the reference case (see Section 3.2). Therefore, the number of vitrified waste generations is 20 % lower than that in the reference case. For various cooling times, the repository footprints in the reference and increased-waste content cases were determined by thermal calculations. with variable cooling time, and the results are listed in Tables 7 and 8, respectively In the original disposal scenario, increasing the waste content increases the footprint from 40.0 m^2 to 66.0 m^2. Despite the lower number of waste package generations, the total footprint of the waste packages also exceeds the reference case. However, owing to the rapid heat decay of the FPs, the footprint can be minimized by extending the cooling time by 30 years and 40 years in the reference case and waste-content increased case, respectively. It is notable that the minimum footprint is determined only by structural limitations. In addition, the criticality is not problematic because the waste includes no fissile materials.

Tables7 and 8

5. Optimization with Partitioning Technology

5.1 Significance and Conditions for Partitioning

Partitioning technology has been developed by JAEA as a part of P&T technology to reduce the environmental burden of HLW. (Oigawa, 2012) In the concept so-called double strata transmutation system, the transmutation cycle is clearly divided from the fuel cycle of power generation. The transmutation is performed by Accelerator Driven System (ADS), which can convert a large amount of Minor Actinoid (MA) because a large amount of loading MA around 60 wt%IHM in the fuel. The ADS transmutation compacts the scales of the transmutation cycle. The transmutation system can connect to any fuel cycle of power generation, including an HTGR. Therefore, combining the HTGR fuel cycle with the double strata transmutation system is a feasible future option. It is said that this system reduces the repository footprint of HLW to 1/100 that of the representative reprocessing case discussed in Section 4.2. On the contrary, this system requires many innovative technologies that are not yet developed, for example, sourcing neutrons by the nuclear spallation reaction, a Pb-Bi cooled fast reactor core, and pyro-reprocessing. From an early introduction perspective, another option without transmutation should be proposed.

The double strata transmutation system uses a partitioning technology called four-group partitioning. New partitioning technology (Morita, 2009) have been also developed to reduce solvent wastes by the “CHON,” principle which means usage of chemical reagent composition of elements C, H, O and N, exclusively because solvent including phosphate, such as TriButyl Phosphate (TBP), cannot be incinerated and is disposed of as solidified wastes in general. However, the partitioning specifications are not significantly changed in this new technology because they mainly depend on the process design, such as the number of cascades. Here, we evaluate the effectiveness of a modified four-group partitioning in reducing HLW. To reduce the number of vitrified

waste forms, four-group partitioning divides the nuclides in the High Level Liquid Waste (HLLW) into four groups: the PGMs group, the Sr-Cs group, the MAs group (Np, Am, Cm), and others group. In this study, the MAs are placed into the others group. As described in Section 3.1, the fabrication of vitrified waste must limit the amount of PGMs and the decay heat, which is dominated by Sr-Cs groups. Therefore, the group partitioning alleviates the technical difficulties of vitrified waste fabrication. Moreover, the others group is contained into the "high-waste-loading glass" (Yoneyama, 1995; Nishihara, 2010), which contains up to 35 wt% of waste oxide and 8 wt% of MoO_3. The nuclides of the Sr-Cs groups are absorbed in the partitioning process, and their absorbers stabilized as Sr-Cs calcined waste forms by mixing and heating. For disposal purposes, the dimensions of the calcined forms are designed to match those of the vitrified waste (Nishihara, 2010). The specifications of the waste forms are listed in Table 9.

Although the Sr–Cs calcined waste generates most of the decay heat, Sr-Cs is not the transmutation target. The only feasible option is storing the calcined waste form to reduce its decay heat before disposal. The double strata transmutation system operates in either the long-term scenario or super-long-term scenario which extends the cooling time of the Sr–Cs calcined waste to 130 and 300 years, respectively, and reduces the repository footprint to 1/4 and 1/100 that of the representative reprocessing scenario, respectively. When deciding between the long-term scenario and the super-long-term scenario, we should consider the acceptability of the 300 years cooling time. Another difficulty in the super-long-time scenario is the compact emplacement of the disposal (see Fig.8). The compact emplacement concept was originally proposed for disposal of Low Level Waste (LLW) (JNC, 2000b), whose decay heat is negligibly

smaller than that of the HLW. The four canisters are solidified by cement, and the piled up cement cubes are surrounded by buffer material. For disposal with compact emplacement, the MAs should be separated from the vitrified waste, and the Sr-Cs calcined waste should be cooled over 300 years.

To enable early introduction of our waste disposal scheme, we employ partitioning technologies under the following conditions.

- The Sr-Cs group is separated and disposed of as a calcined form.
- The PMGs group is separated and reused.
- Other nuclides, including the MAs (Np, Am, Cm), are vitrified and disposed of as high-loading glass waste forms.
- The pre-disposal cooling time is 150 years.

Table 9 and Fig.8

5.2 Number of Waste Packages and Repository Footprint with Partitioning

The number of generated waste packages and other properties of the vitrified and Sr-Cs calcined waste forms are listed in Table 10. With margins for other limitations, the number of waste packages is determined by the limited waste-oxide content. There are margins for other limitations. In this analysis, the Sr and Cs calcined forms are individually evaluated to elucidate their characteristics although they are mixed and solidified in actual disposal. The partitioning reduces the number of vitrified waste packages by 80% (from 2.32 canister/TWeh in the representative case to 0.502 canister/TWeh with partitioning). Including the Sr-Cs calcined waste package, partitioning reduces the number of waste packages by 60 % (to 0.833 canister/TWeh).

The repository footprint of each waste form is evaluated with horizontal emplacement and a post-partitioning cooling time of 150 years. Figure 9 plots the

maximum bentonite temperature after disposal. The repository layout of the Sr and Cs calcined wastes is set to minimize the footprint at 20.3 m^2/canister. Within the structural limitations, the required canister pitch and drift interval are 3.5 m and 5.8 m, respectively. In the closest emplacement scheme, the bentonite temperatures of the Sr and Cs calcined wastes are 88.3 °C and 82.3 °C, respectively, at 30 years after disposal. However, the temperature of the vitrified waste with the minimum footprint exceeds the limit of 90 °C. After extending the canister pitch and drift interval to 5.0 m and 7.0, respectively, the footprint increases to 35.0 m^2/canister, but the maximum bentonite temperature of the vitrified waste is 84.1 °C at 300 years after disposal. With a half-life of 432 years, most of the decay heat comes from ^{241}Am and is difficult to reduce by cooling. Therefore, to reduce more the footprint of the vitrified waste within the temperature limit, P&T of the MAs is required. The evaluated specifications of the waste disposal are summarized in Table 11. In addition, the criticality is not problematic because the waste includes no fissile materials.

Tables10,11 and Fig.9

6. Consideration on Optimized HLW Specifications and Reduction Effect with Partitioning

Table 12 and 13 summarize the main result of Section 4 and our previous study, respectively, in direct disposal and disposal with reprocessing. In direct disposal and horizontal displacement with no scenario change, the small structural limitation of the drift peach reduces the repository footprint by 20 %. Extending the cooling time by 20 and 40 years reduces the footprint by 40 % and 50 %, respectively, in relation to the decay of FPs.

Tables 12 and 13

In disposal with reprocessing, horizontal emplacement alone reduces the

footprint by 55% only by employing the horizontal emplacement. Increasing the waste component by 30 % (i.e., increasing the initial heavy metal inventory of SF from 0.330 tIHM/canister to 0.432 tIHM/canister) reduces the number of generated vitrified-waste canisters by 20%. This can be achieved merely delaying the reprocessing by 1.5 years; no process changes and/or innovative reprocessing technologies are required. However, with horizontal emplacement and a cooling time of 54 years, the increased heating increases the footprint per electricity generation from 92.7 m^2/TWeh to 116.7 m^2/ TWeh despite the 20% reduction in number of canisters. To minimize the footprint at 20.3 m^2/canister (77 % lower than the footprint of vertical emplacement) under the structural limitation, the cooling time must be extended by 30 years and 40 years in the reference case and the waste-content increased case, respectively. The footprint per unit of electricity generation is reduced by ~80 % (77 % and 82 % in the reference case and the waste-content increased case, respectively), from that of vertical emplacement.

The specifications of disposal with reprocessing and partitioning are summarized in Table 14. The total number of waste packages is 60% lower than that in the representative reprocessing case. The repository footprint per electricity generation is reduced by 90 %. Table14

Next, we discuss the acceptability of the disposal scenarios and the designed method. In the optimized scenario, we assess the reduction of the repository footprint by extending the cooling time by 40 years. This cooling term is certainly acceptable because delay of the plan of the nuclear fuel cycle is compatible with this term due to delay in the operation of the Rokkasho Reprocessing Plant (RRP) in Japan. The cabinet office, government of Japan reevaluated the cost of electricity generation after the Fukushima Daiichi nuclear power plant disaster (Committee of Electricity Generation

Cost Verification, 2011) and developed a new scenario reflecting the current state of nuclear fuel cycle in Japan. This scenario divides the SFs into two equal parts, one part to be reprocessed at 20 years post-discharge, the remainder to be reprocessed after 50 years. The average cooling time before reprocessing is 35 years, which is compatible with the 40 years delay in the proposed scenario.

On the contrary, partitioning with a cooling time of 150 years is much longer than the operation fluctuations in the nuclear fuel cycle. Nevertheless, such a long cooling time might be justified by the long schedule of geological disposal and public willingness. The planned time of monitoring is 300 years after closure of the repository (JAEC, 2004). The objectives are to provide information for making management decisions, system behavior from the viewpoint of safety and public acceptance, and to maintain nuclear safeguards for direct disposal. (IAEA, 2001). The management (including monitoring) of HLW should continue for at least 350 years. In addition, the policy of geological disposal of HLW promoted by the Nuclear Waste Management Organization of Japan (NUMO) has been criticized by the Science Council of Japan (SCJ), which was selected by JAEC as the third-party opinion source for HLW disposal in NPG. The opinions of the SCJ, distilled in their report entitled “Issues concerning HLW Disposal (Reply)” (SCJ, 2012) in 2012, can be regarded as the public willingness. In the report requested by the JAEC, the SCJ recommended the research and development of P&T and disposal with Reversibility and Retrievability (R&R). The public will willingly accept a long-term scenario. However, in Japan, the disposal site cannot be determined, and long-term storage is the publicly acceptable final disposal mode. The cooling time of 150 years would be limitation to be accepted, we believe.

Finally, we discuss the burdens of storage. In simple terms, extending the

cooling time reduces the repository footprint, but it requires a large storage facility. In this context, the footprint of each disposal method is measured by the storage capacity index defined as the product of the storage area and storage term (Nishihara et al. 2010). P&T including MA transmutation can diminish the footprint and maintain a small storage capacity index (Nishihara et al. 2010). The storage burdens are public acceptance and economy. Public acceptance is not problematic considering that the SF storage facilities which have operated even in Japan, unless it is not regarded as final disposal due to the long storage term. The only real storage burden is the economy of disposal. Table 15

To determine the economic burden of storage, the relation between cost and extended cooling time is assessed in numerical experiments. The unit back-end costs in the direct disposal of LWR SFs have been evaluated by the cabinet office of the Government of Japan and are listed in Table 15. Using these unit costs, the back-end cost is converted to the Net Present Value (NPV) at the time of SFs generation by discounting and summing. The discounting technique is the *de facto* standard method for evaluating the costs and benefits for NPG (OECD, 1994). The unit costs are also evaluated with the discounting technique by dividing the NPV of the cost by the NPV of processed SFs amount. The storage and disposal costs are incurred early by depreciation of the construction cost. The SFs of storage and disposal are performed during the operation. The amount of processed SFs is reduced lesser than the costs with higher discount rate. In this study, the discounted back-end cost of direct disposal of LWR SFs is evaluated by the continuous discounting method.

First the discount rate is converted to a continuous discount rate as follow,

$$r' = \ln(1 + r) \quad , \tag{1}$$

where,

r: discount rate (-),

r': continuous discount rate (-).

The cost rate of storage is evaluated by assuming a constant rate for the storage term, and evaluating the following integral:

$$P_{strage} = \int_0^{T_s} R_{strage} \exp(-r'(t - T_D))\, dt \quad , \tag{2}$$

where,

P_{strage}: unit cost of storage (million yen/tU),

R_{strage}: cost rate of storage (million yen/tU·year),

T_S: storage term (year),

T_D: representative time for discounting (year).

To evaluate the cost rates, we assume the unit storage costs for each discount rate given in Table 15, and a storage term of 50 years. The representative term of discounting is the approximate middle of the storage time (Yamaji, 2004). Applying the cost rate and Eq. (2), we can evaluate the continuous unit cost of storage for an arbitrary storage term. The contentious storage cost generation is treated by the JALTES-II code (Sato, 1985), which computes the economics of NPG. SFs are cooled for 4 years in the SF pool of a Nuclear Power Plant (NPP), then transported to an interim storage facility, and stored. In the calculations, the storage term is varied from 50 to 500 years. After storage, the SFs are transported to a geological repository, where they are disposed of. Finally, the

back-end cost is calculated follows,

$$\mathrm{TotalCost} = P_{\mathrm{transport1}} \exp(-r'T_1) + \int_0^{T_2} R_{\mathrm{strage}} \exp(-r'(t+T_1))\,dt + P_{\mathrm{transport2}} \exp(-r'(T_1+T_2)) + P_{\mathrm{disposal}} \exp(-r'(T_1+T_2)) \quad , (3)$$

where,

T_1: time from discharge to transport (year),

T_2: storage term (year),

$P_{\mathrm{transport1}}$: unit cost of transport from NPP to storage facility (million yen/year),

$P_{\mathrm{transport2}}$: unit cost of transport from storage facility to geological repository (million yen/year),

P_{disposal}: unit cost of disposal (million yen/year).

The terms in right hand side corresponds to the cost of transport from NPP to storage facility, the cost of storage, the cost of transport from storage facility to repository, and the cost of disposal, respectively. When the storage term approaches infinity, the cost of transport from the storage facility to the repository and the cost of disposal cost both diminish to zero. Consequently, the total cost approaches a certain value with non-zero discount rate as follows,

$$\lim_{T_2 \to \infty} \mathrm{TotalCost} = P_{\mathrm{transport1}} \exp(-r'T_1) + \frac{R_{\mathrm{strage}}}{r'} \exp(-r'T_1) \quad . (4)$$

The result is shown in Fig. 10. When the discount rate is zero, the total cost increases with increasing storage term because of the increased storage cost. On the contrary, when the discount rates are non-zero, the total cost decreases with increasing cooling term and approaches the value given by Eq. (4). The asymptotic value reduces as the discount rate increases. This result does not reflect the effect of reducing the footprint

and technical difficulty of reducing the decay heat.

In the optimized system, extending the cooling time can reduce the cost of long cooling terms as confirmed above. A similar situation was reported by the cabinet office of the government of Japan, who evaluated the cost of electricity generation by the NNP. After revising the above scenario to account for the scheduling delay of the RRP operation, the back-end cost is reduced by 0.6 yen/kWh, with a discount rate of 3 %.

As the problem concerns the long-term costs and benefits, it must also accommodate climate change (or global warming), because the abatement cost should reasonably compare with the predicted damage cost at infinite time. The so-called "Stern review" has been influential in this field (Stern, 2007). Stern concluded that the cost of reducing greenhouse gas emissions will approximate 1 % of the global Gross National Product (GDP). If climate change is ignored, the damage cost to GDP increases to 5-20 %. The evaluation assumes a low discount rate of 1.4 %. The discount rate is a commonly used parameter in this field (Committee on Health, Environmental, and Other External Costs and Benefits of Energy Production and Consumption, et al. 2010). In general, the discount rate is evaluated according to Ramsey's approach (Ramsey, 1928), derived by optimizing the long-term saving, as follows,

$$r = \rho + \theta g \quad , \tag{5}$$

where,

ρ: pure time preference (-),

θ: consumption elasticity of marginal utility (-),

g: economic growth rate (-).

Stern set the pure time preference, consumption elasticity of marginal utility, and the economic growth rate to 0.1%, 1.0, and 1.3%, respectively. Weitzman suggested that more plausible values are approximately 2 %, 2.0, and 2 %. (Weitzman, 2007a and 2007b), which increase the discount rate to 6 %. Nordhaus adopted a Fig.10 e approach, calibrating his model parameters to match the discount rate to the market interest rate. (Nordhaus, 2008) His obtained discount rate was 4.5 %. Even at the lowest discount rate derived by Stern (1.4%), lengthening the storage term lowers the cost. According to the discounting analysis, the long storage term and/or large storage capacity index is not economically burdensome.

7. Conclusions

In the previous study, the footprint of geological repository of HTGR was evaluated with the vertical emplacement based on the KBS-3V concept, and smaller repository footprint is expected with the horizontal emplacement based on the KBS-3H concept and optimizing disposal scenario.

The burn-up fuel composition of the HTGR was evaluated by ORIGEN code using the ORIGEN library for HTGR generated in a previous study. The geological repository design, which must limit the maximum bentonite temperature, was determined by thermal calculation in ANSYS code. The criticality safety was assessed by MVP code.

Without any scenario change, the horizontal emplacement reduces the repository footprint of direct disposal by 20%. The footprint can be further reduced by extending the cooling time. Specifically, extending the cooling time by 20 and 40 years

reduced the footprint by 40 % and 50 %, respectively.

In disposal with reprocessing, the horizontal emplacement alone reduced the footprint by 55%. Moreover, increasing component by 30 % in the vitrified waste reduced the number of generated waste canister by 20 %, and required only a 1.5 year reprocessing delay. Extending the cooling time by 30 and 40 years reduced the footprint per unit of electricity generation by 77 % and 82 %, respectively.

In disposal with reprocessing and partitioning, the total number of waste packages was 60% lower than in the representative reprocessing case. The repository footprint per unit of electricity generation was reduced by 90 % after a cooling time of 150 years.

The acceptability of the disposal scenario and designed method was also discussed. The extended cooling time by 40 years in the optimized scenarios is acceptable because it approximates the planning delay of the nuclear fuel cycle in Japan. In disposal with reprocessing and partitioning, the 150 years cooling time is potentially acceptable given the long planning time of HLW management and the public willingness of R&R. Long-term storage does not increase the back-end cost; rather, numerical experiments demonstrated that increasing the cooling time lowers the cost.

Acknowledgement

The authors appreciate Dr. J. Sumita of JAEA who is an expert in back-end of HTGR, and provided valuable comments.

References

ANSYS, Inc. 2013. ANSYS Mechanical APDL Theory Reference. ANSYS, Inc.

Committee of Electricity Generation Cost Verification, 2011. Committee of Electricity Generation Cost Verification Report:19th. Cabinet Secretariat of Japan. [in Japanese]

Committee on Health, Environmental, and Other External Costs and Benefits of Energy Production and Consumption, Board on Environmental Studies and Toxicology, Division on Earth and Life Studies, Board on Energy and Environmental Systems, Division on Engineering and Physical Sciences, Board on Science, Technology, and Economic Policy, Policy and Global Affairs Division. 2010. Hidden Cost of Energy: Unpriced Consequence of Energy Production and Use. The National Academies Press.

Croff, A. G. 1983. ORIGEN2: A Versatile Computer Code for Calculating the Nuclide Compositions and Characteristics of Nuclear Material. Nucl. Technol.,62, 335-352.

Fukaya Y., Nishihara T., 2016. Reduction on High Level Radioactive Waste Volume and Geological Repository Footprint with High Burn-up and High Thermal Efficiency of HTGR. Nucl. Eng. Des., 307, 188-198.

International Atomic Energy Agency (IAEA). 2001. Monitoring of geological repositories for high level radioactive waste. International Atomic Energy Agency. IAEA-TECDOC-1208.

Inagaki, Y., Iwasaki, T., Sato, S., et al. 2009. LWR High Burn-Up Operation and MOX Introduction; Fuel Cycle Performance from the Viewpoint of Waste Management. J.

Nucl. Sci. Technol. 46(7), 677-689.

Japan Atomic Energy Commission (JAEC). 2004. Report on comparison of nuclear fuel cycle cost in the basic scenario. Japan Atomic Energy Commission. URL: http://www.aec.go.jp/jicst/NC/iinkai/teirei/siryo2004/kettei/sakutei041124.pdf [in Japanese].

Japan Nuclear Cycle Development Institute (JNC). 2000a. Second Progress Report on Research and Development for the Geological Disposal of HLW in Japan; H12: Project to Establish the Scientific and Technological Basis for HLW Disposal in Japan, Project Overview Report, Japan Nuclear Cycle Development Institute, JNC TN1410 2000-001.

Japan Nuclear Cycle Development Institute (JNC), Federation of Electric Power Companies, 2000b. Progress Report on Disposal Concept for TRU Waste in Japan, Japan Nuclear Cycle Development Institute, JNC TY1400 2000-002.

Koning, A. J., Bauge, E., Dean C. J., et al. 2011a. Status of the JEFF Nuclear Data Library. J. Korean Phys. Soc., 59 (2), 1057-1062.

Koning, A. J., Forrest, R., Kellett, M., et al. 2006. The JEFF-3.1 Nuclear Data Library. France: Nuclear Energy Agency, Organization for Economic Co-operation and Development, JEFF Report 21.

Koning, A. J., Rochman, D., 2011b. TENDL-2011:TALYS-based Evaluated Nuclear Data Library. URL:http://www.talys.eu/

Morita, Y., Sasaki, Y., Asakura, T., et al., 2010. Development of a new extractant and a new extraction process for minor actinide separation. IOP Conference Series; Materials Science and Engineering, 9, 012057_1 - 012057_11.

Murata, I., Takahashi, A., Mori, T., et al., 1997. New Sampling Method on Continuous Energy Monte Carlo Calculation for Pebble Bed Reactors. J. Nucl. Sci. Technol. 34(8), 734-744.

Nakata, T., Katanishi, S., Takada, S., et al. 2003. Nuclear, thermal and hydraulic design for Gas Turbine High Temperature Reactor (GTHTR300). J. At. Energy Soc. Jpn. 14(3). [in Japanese]

Nakajima, Y., 1991. JNDC WG on Activation Cross Section Data: “JENDL Activation Cross Section File”. Proc. the 1990 Symposium on Nuclear Data. Japan Atomic Energy Research Institute, JAERI-M 91-032, 43-57.

Nagaya, Y., Okumura, K., Mori, T., 2006. A Monte Carlo neutron/photon transport code MVP 2, Trans. Am. Nucl. Soc. 95, 662-663.

Nishihara, K., Oigawa, H., Nakayama, S., et. al., 2010. Impact of Partitioning and Transmutation on High-Level Waste Disposal for the Fast Breeder Reactor Fuel Cycle, . Nucl. Sci. Technol., 47(12), 1101-1117.

Nordhaus, W.D. 2008. A Question of Balance: Weighing the Options on Global Warming Policies. Yale University Press.

Organization for Economic Co-operation and Development (OECD). 1985. The Economics of the Nuclear Fuel Cycle. Organization for Economic Co-operation and Development.

Organization for Economic Co-operation and Development (OECD). 1994. The Economics of the Nuclear Fuel Cycle. Organization for Economic Co-operation and Development.

Organization for Economic Co-operation and Development (OECD). 2002. Accelerator-driven Systems (ADS) and Fast Reactors (FR) in Advanced Nuclear Fuel Cycles: A Comparative Study, Organization for Economic Co-operation and Development.

Okumura, K., Sugino, K., Koshima, K., et al. 2012. A Set of ORIGEN2 cross section libraries based on JENDL-4.0; ORLIBJ40. Japan Atomic Energy Agency, JAEA-Data/Code 2012-032.

Ohashi, H., Sato, H., Tachibana, Y., Kazuhiko K., and Ogawa, M., 2011. Concept of an Inherently-safe High Temperature Gas-cooled Reactor. ICANSE 2011, 50-58.

Oigawa, H., 2012. Present status and prospect of transmutation technology for high-level radioactive waste. Radioisotopes, 61, 571-586.[in Japanese]

Ramsey, F. P. 1928. A Mathematical Theory of Saving. The Economic Journal. 38(152), 543-559.

Sato, O., Yasukawa, S., 1985. JALTES-II: A System Analysis Model for Long-Term Strategy on Nuclear Power Development, Japan Atomic Energy Agency, JAERI-M 85-129. [in Japanese]

Science Council of Japan (SCJ). 2012. Issues concerning HLW Disposal (Reply). Science Council of Japan.
URL: http://www.scj.go.jp/ja/info/kohyo/pdf/kohyo-22-k159-1.pdf

Shibata, K., Iwamoto, O., Nakagawa, T., et al. 2011. JENDL-4.0: A New Library for Nuclear Science and Engineering. J. Nucl. Sci. Technol. 48(1), 1-30.

Stern, N. 2007. The Economics of Climate Change: The Stern Review. Cambridge University Press.

Svensk Kärnbränslehantering AB (SKB), 2010. Spent nuclear fuel for disposal in the KBS-3 repository. Svensk Kärnbränslehantering AB, Technical Report TR-10-13.

Weitzman, M. L. 2007a. Structural Uncertainty and the Value of Statistical Life in the Economics of Catastrophic Climate Change. National Bureau of Economic Research, Inc., NBER Working Paper No. W13490.

Weitzman, M. L. 2007b. A review of the “Stern Review on the Economics of Climate Change” J. Econ. Lit. 45(3),703-724.

Yamaji, K., 2004. FCOST-UT. the university of Tokyo.
URL: http://www.iwafunelab.iis.u-tokyo.ac.jp/yamaji/index_j.html

Yan, X., Kunitomi, K., Nakata, K., et al., 2003. GTHTR300 design and development. Nucl. Eng. Des. 222, 247-262.

Yoneya, M., Kawamura, K., Igarashi, H., et al., 1995. Technical incentive to high-waste-loading process of HLLW. Proc. 5th Int. Conf. on Radioactive Waste Management and Environmental Remediation—ICEM’95, Berlin, Germany, Sep. 3–7, 1, 389–393.

List of Tables and Figures

Fig.6 Maximum bentonite temperature versus disposal time in direct disposal with various extended cooling times

Fig.7 Temporal criticality changes in the repository with and without FPs

Fig.8 Concept of compact emplacement

Fig.9 Maximum bentonite temperature with partitioning

Fig.10 Total back-end costs as functions of storage term at terms discount rates

Table 1 Main specifications of GTHTR300

Item	Value
Thermal power (MWt)	600
Thermal efficiency (%)	45.6
Uranium inventory (t)	7.09
^{235}U enrichment (wt%)	14
Fuel particle	SiC coated particle
Kernel diameter (μm)	550
Particle diameter (μm)	1,010
Particle packing fraction (%)	28.5
Block across flat (mm)	410
Fuel rod numbers	57
Fuel rod diameter (mm)	26
Coolant hole diameter (mm)	39
Burnable poison	B4C-C composite
Block height (mm)	1,050
Cycle length (days)	706.0
Number of batch	2
Discharge burn-up (GWd/t)	119.5
Initial heavy metal inventory per electricity generation (tIHM/TWeh)	0.765

Table 2 Conditions of the burn-up calculations

	PWR	HTGR
Enrichment (wt%)	4.5	14
Specific power (MW/t)	38	84.63
Burn-up days (day)	1184.21	1412.09
Burn-up (GWd/t)	45	119.5

Y. Fukaya:
Optimization of Disposal Method and Scenario to Reduce High Level Waste Volume and Repository Footprint for HTGR

Table 3 Specifications of waste package and its repository evaluated in the previous study (Fukaya, et al. 2016)

	PWR		HTGR
Specifications			
Burn-up (GWd/t)	45		119.5
Thermal efficiency (%)	34.5		45.6
Initial heavy metal inventory per electricity generation (tIHM/TWeh)	2.684		0.765
	2 assemblies in a canister	4 assemblies in a canister	
Direct disposal			
Initial heavy metal inventory of spent fuel per canister (tIHM /canister)	0.920	1.840	0.639
Number of canisters per electricity generation (canister/TWeh)	2.92	1.46	1.20
Repository footprint per canister (m^2/canister)	192	320	204
Repository footprint per electricity generation (m^2/TWeh)	560.1	466.8	244.0
Disposal with reprocessing			
Initial heavy metal inventory of spent fuel per canister (tIHM/canister)	0.790		0.330
Number of canisters per electricity generation (canister/TWeh)	3.40		2.32
Repository footprint per canister (m^2/canister)	90		90

Repository footprint per electricity generation (m^2/TWeh)	305.8	208.5

Y. Fukaya:
Optimization of Disposal Method and Scenario to Reduce High Level Waste Volume and Repository Footprint for HTGR

Table 4 Main specifications and limitations for the Japanese vitrified waste model

Items	Values
Materials	
Matrix	Borosilicate glass
Canister	Stainless steel
Dimensions	
Diameter (mm)	430
Height (mm)	1,340
Weights	
Glass (kg/canister)	400
Glass including canister (kg/canister)	500
Volume of glass (liter/canister)	150
Vitrification melter type	Liquid Fed Ceramic Melter (LFCM)
Limitations	
Heat generation rate for storage period (kW/canister)	＜ 2.3
Waste oxides content (wt%)	＜ 20
MoO_3 content (wt%)	＜ 1.5
PGM content (wt%)	＜ 1.25

Table 5 Optimization of vitrified waste specifications for the HTGR

	Reference case	Optimized case	Limitations
Initial heavy metal inventory of SF per canister (tIHM/canister)	0.33	0.43	-
Heat generation at vitrified form fabrication (kW/canister)	2.3	2.2 (3.0*)	< 2.3
Waste oxide content (wt%)	8.6	11.3	< 15.0
MoO_3 content (wt%)	1.1	1.5	< 1.5
PGM content (wt%)	0.8	1.1	< 1.25

*Heat generation in the parentheses is evaluated with no scenario change.

Y. Fukaya:
Optimization of Disposal Method and Scenario to Reduce High Level Waste Volume and Repository Footprint for HTGR

Table 6　Repository footprint in direct disposal with various cooling times

Cooling time from discharge (year)	Extended cooling time from reference case (year)	Footprint (m^2)	Canister pitch (m)	Drift interval (m)	Maximum bentonite temperature (°C)
54	0	160.0	10.0	16.0	90.6
64	10	135.0	9.0	15.0	88.9
74	20	117.0	9.0	13.0	88.5
94	40	104.0	8.0	13.0	87.5

Table 7 Repository footprint of disposal with reprocessing in the reference case

Cooling time from discharge (year)	Extended cooling time from reference case (year)	Footprint (m^2)	Canister pitch (m)	Drift interval (m)	Maximum bentonite Temperature (°C)
54	0	40.0	5.0	8.0	89.5
64	10	30.0	5.0	6.0	88.0
74	20	24.0	4.0	6.0	86.0
84	30	20.3	3.5	5.8	82.3

Table 8 Repository footprint in disposal with reprocessing and increased waste content

Cooling time from discharge (year)	Extended cooling time from reference case (year)	Footprint (m^2)	Canister pitch (m)	Drift interval (m)	Maximum bentonite Temperature (°C)
54	0	66.0	6.0	11.0	90.3
64	10	48.0	6.0	8.0	85.3
74	20	35.0	5.0	7.0	85.6
94	40	20.3	3.5	5.8	86.8

Table 9 Specifications of high-loading glass and Sr-Cs calcined waste forms

	Vitrified waste	Sr-Cs calcined waste	
	(High-loading glass)	Sr	Cs
Volume (m^3)	0.143	0.143	
Weight (kg)	400	-	
Density (g/cm^3)	2.8	4.2	2.47
Waste oxide content (wt%)	< 35.0	< 9.9	< 14.3
MoO_3 content (wt%)	< 8.0	-	
Heat generation rate for storage period (kW/canister)	< 2.3	< 10.0	

Y. Fukaya:
Optimization of Disposal Method and Scenario to Reduce High Level Waste Volume and Repository Footprint for HTGR

Table 10 Number of waste form and heat generation of vitrified waste and Sr-Cs calcined waste forms

	Vitrified waste	Sr-Cs calcined waste	
	(High-loading glass)	Sr	Cs
Initial heavy metal inventory of spent fuel per canister (tIHM/canister)	1.53	5.02	4.29
Number of canister per electricity generation (canister/TWeh)	0.502	0.153	0.178
Waste-oxide content (wt%)	35.0	9.9	14.3
MoO_3 content (wt%)	6.6	-	-
Heat generation rate for storage period (kW/canister)	2.24	6.42	8.13

Y. Fukaya:
Optimization of Disposal Method and Scenario to Reduce High Level Waste Volume and Repository Footprint for HTGR

Table 11 Repository specifications of waste with partitioning

	Vitrified waste	Sr-Cs calcined waste	
	(High-loading glass)	Sr	Cs
Canister pitch (m)	5	3.5	3.5
Drift interval (m)	7	5.8	5.8
Repository foot print (m^2/canister)	35.0	20.3	20.3
Maximum bentonite temperature (℃)	84.1	88.3	82.3

Y. Fukaya:
Optimization of Disposal Method and Scenario to Reduce High Level Waste Volume and Repository Footprint for HTGR

Table 12 Optimization summary of direct disposal

	Direct disposal			
Disposal method	Vertical	Horizontal	Horizontal	Horizontal
Cooling time (years)	54	54	74	94
Initial heavy metal inventory of spent fuel per canister (tIHM/canister)	0.639	0.639	0.639	0.639
Number of canister per electricity generation (canister/TWeh)	1.20	1.20	1.20	1.20
Repository footprint per canister (m^2/canister)	204.0	160.0	117.0	104.0
Repository footprint per electricity generation (m^2/TWeh)	244.0	191.4	140.0	124.4

Table 13 Optimization summary of disposal with reprocessing

	Disposal with reprocessing				
Disposal method	Vertical	Horizontal	Horizontal	Horizontal	Horizontal
Cooling time (years)	54	54	84	54	94
Initial heavy metal inventory of spent fuel per canister (tIHM/canister)	0.330	0.330	0.330	0.432	0.432
Number of canister per electricity generation (canister/TWeh)	2.32	2.32	2.32	1.77	1.77
Repository footprint per canister (m^2/canister)	90.0	40.0	20.3	66.0	20.3
Repository footprint per electricity generation (m^2/TWeh)	208.5	92.7	47.0	116.7	35.9

Table 14 Summary of disposal with partitioning

	Total waste packages	Vitrified waste (High-loading glass)	Sr-Cs calcined waste	
			Sr	Cs
Disposal method	Horizontal	Horizontal	Horizontal	
Cooling time (year)	154	154	154	
Number of canister per electricity generation (canister/TWeh)	0.833	0.502	0.153	0.178
Repository footprint per canister (m^2/canister)	-	35.0	20.3	
Repository footprint per electricity generation (m^2/TWeh)	24.3	17.6	3.1	3.6

Table 15 Unit back-end cost of LWR in direct disposal

	Discount rate = 0 %	Discount rate = 1 %	Discount rate = 3 %	Discount rate = 5 %
Transport from NPP to reprocessing plant (million yen/tU)	16	16	16	16
Storage (million yen/tU)	36	40	52	69
Transport from storage facility to geological repository (million yen/tU)	16	16	16	16
Direct disposal (million yen/tU)	132	137	174	249

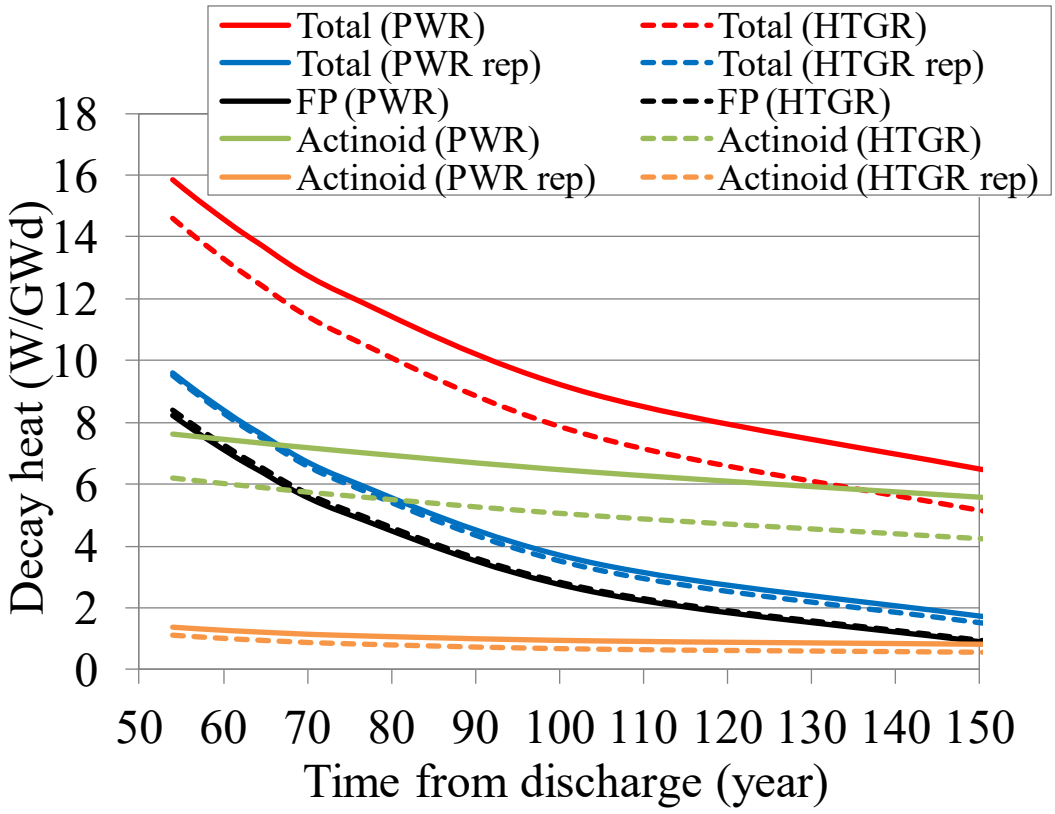

*rep denotes reprocessing.

Fig.1 Decay heat per burn-up of total and constituent wastes as functions of post-discharge time

Y. Fukaya:
Optimization of Disposal Method and Scenario to Reduce High Level Waste Volume and Repository Footprint for HTGR

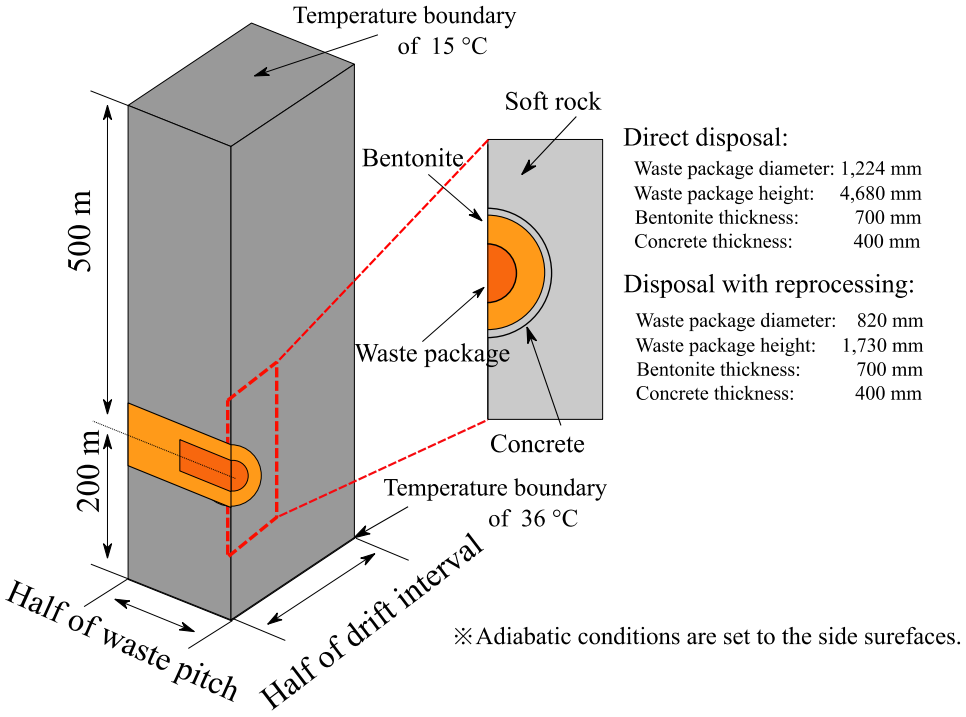

Fig.2 Geometry of horizontal emplacement in the thermal calculation

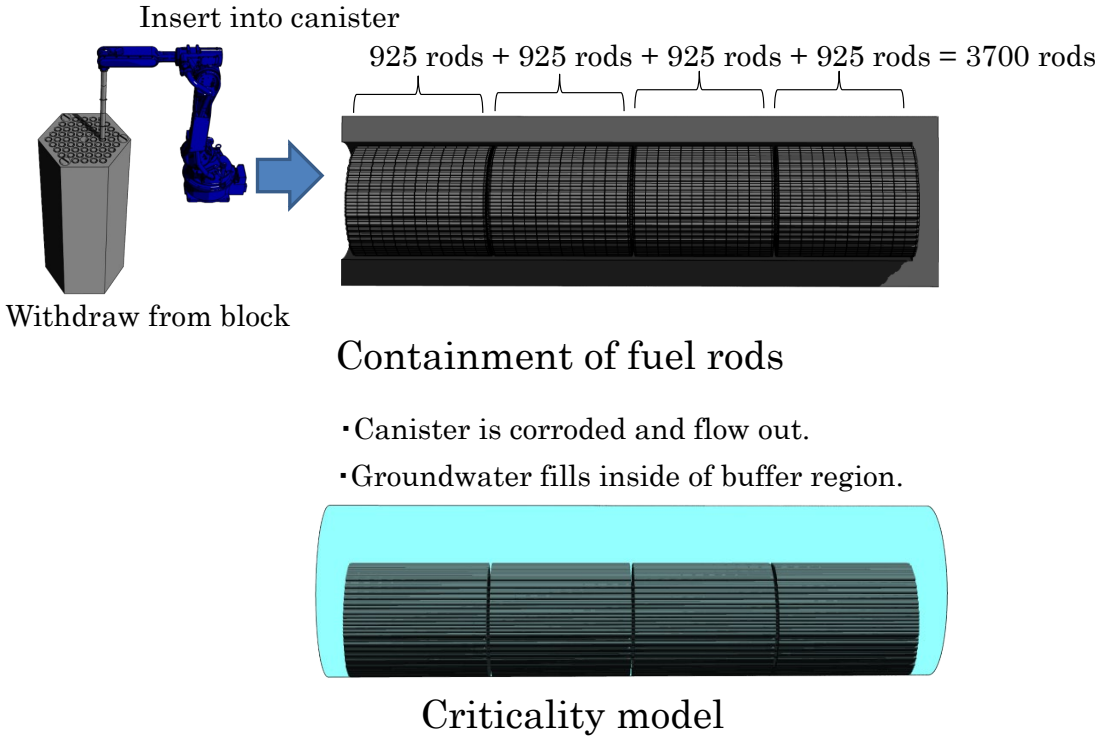

Fig.3 Proposed waste-loading method for HTGR and its criticality model in the repository with horizontal emplacement

Y. Fukaya:
Optimization of Disposal Method and Scenario to Reduce High Level Waste Volume and Repository Footprint for HTGR

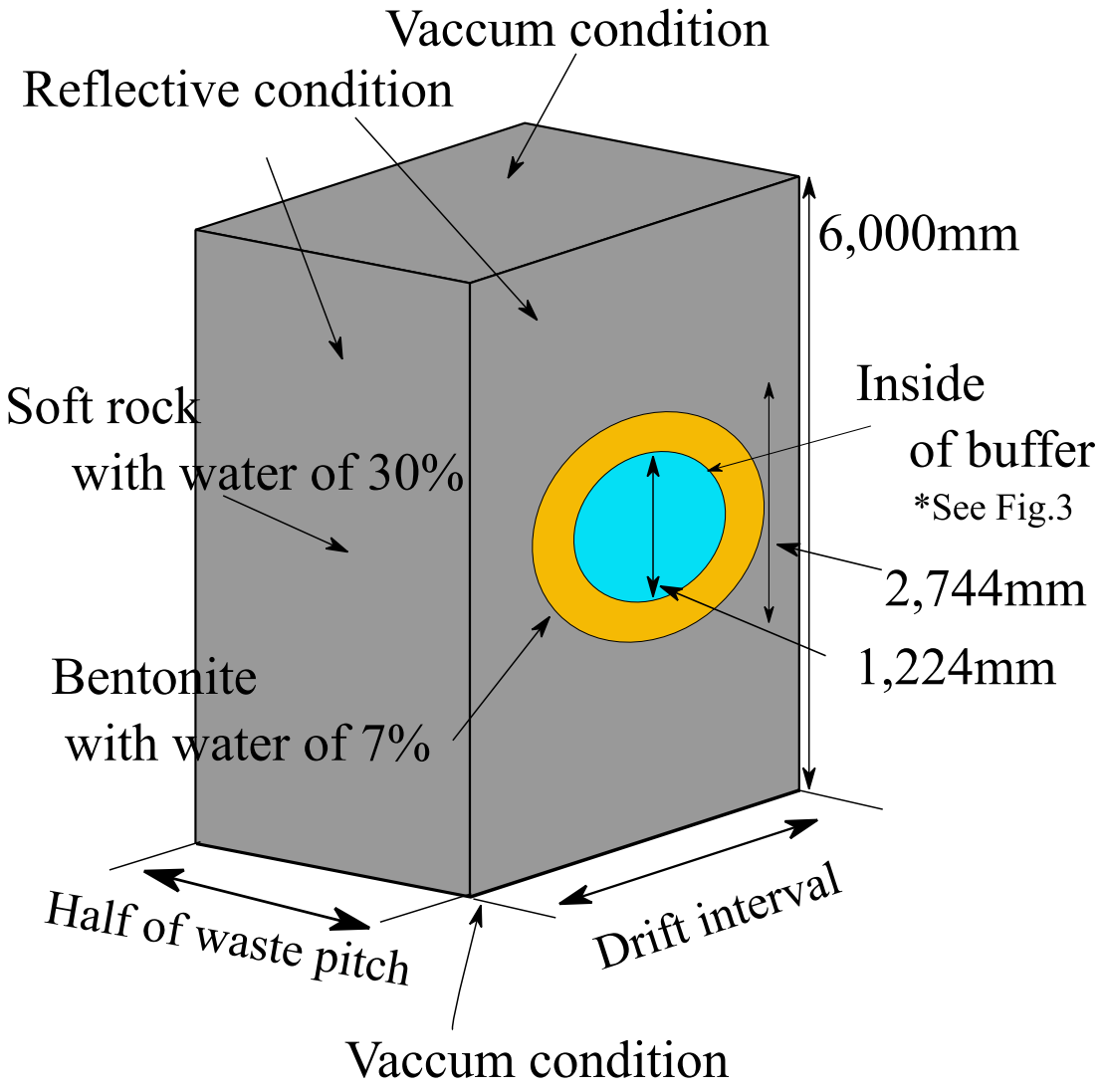

Fig.4 Geometric model of a repository with horizontal emplacement in the criticality calculation

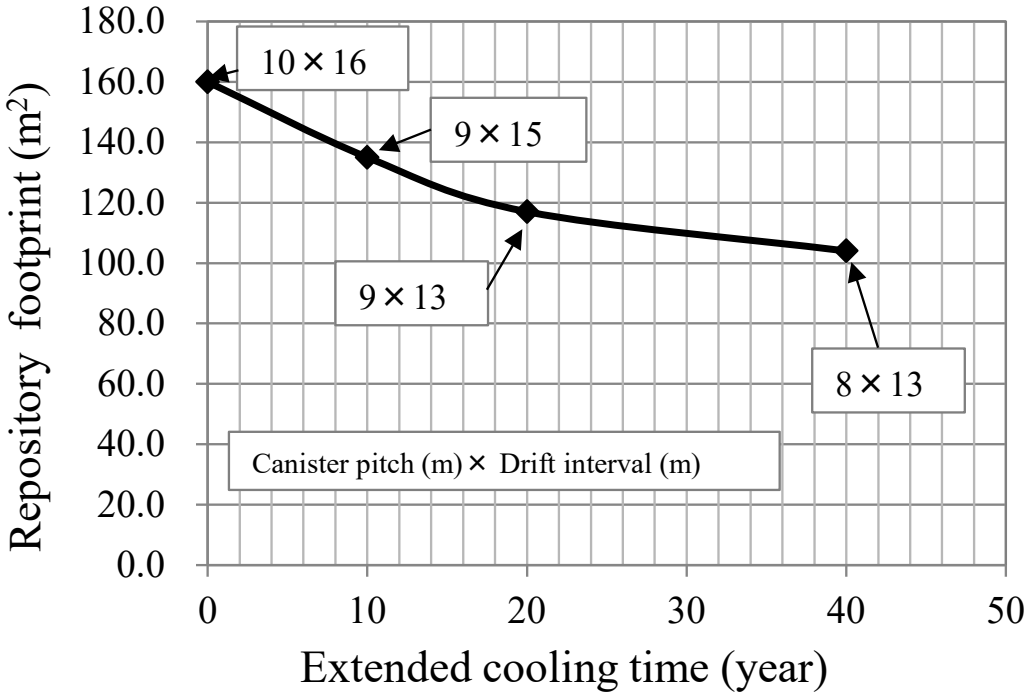

Fig.5 Repository footprint versus cooling time in direct disposal

Y. Fukaya:
Optimization of Disposal Method and Scenario to Reduce High Level Waste Volume and Repository Footprint for HTGR

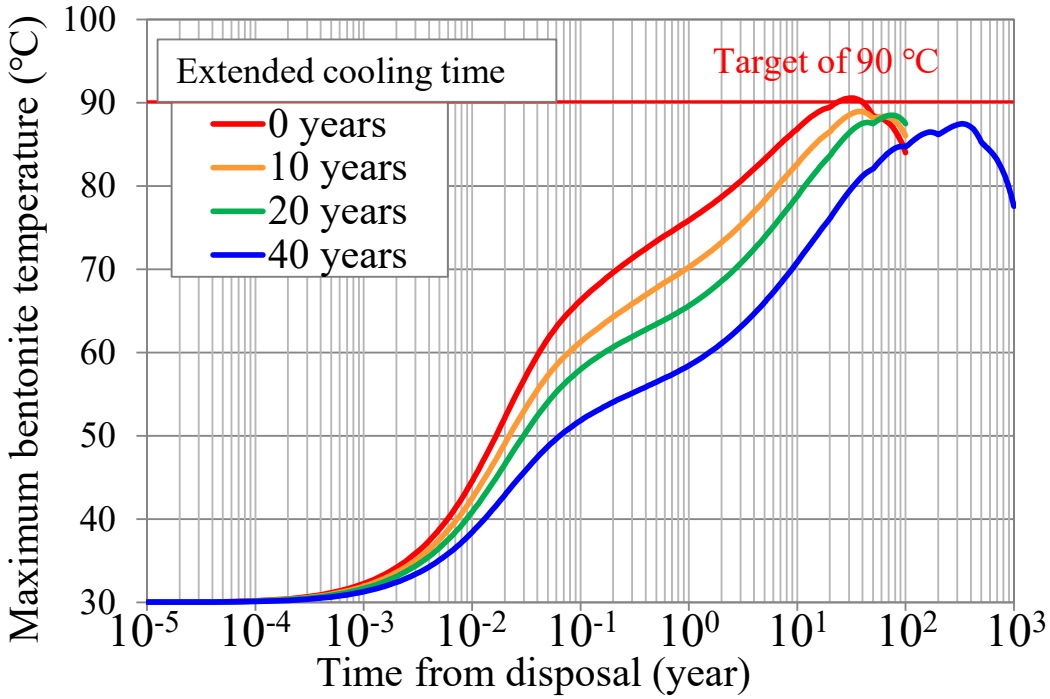

Fig.6 Maximum bentonite temperature versus disposal time in direct disposal with various extended cooling times

Y. Fukaya:
Optimization of Disposal Method and Scenario to Reduce High Level Waste Volume and Repository Footprint for HTGR

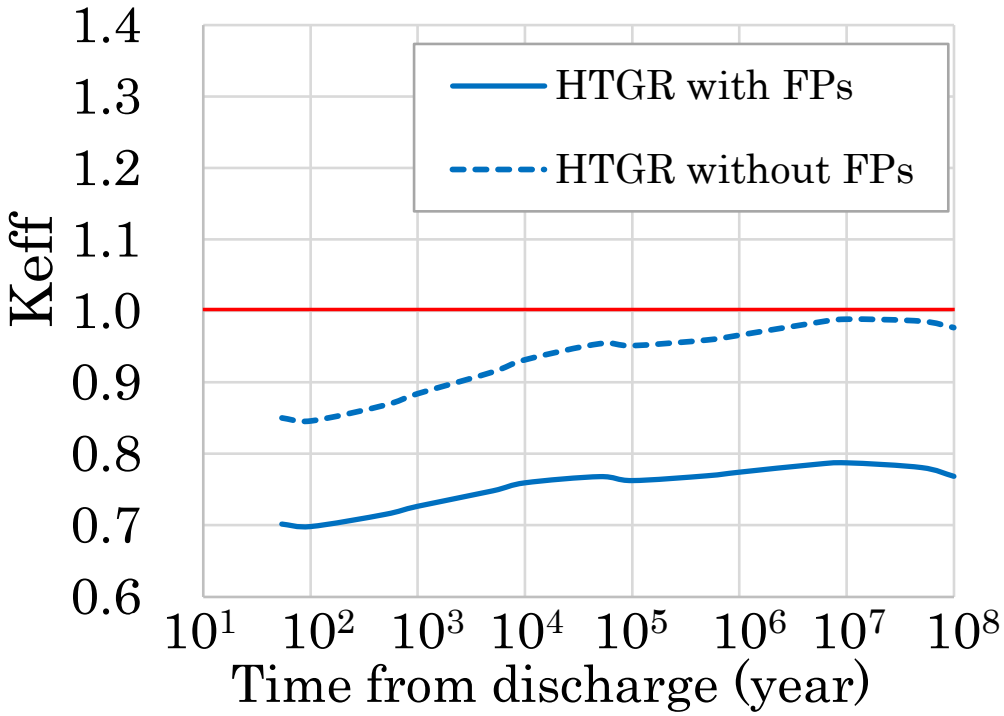

Fig.7 Temporal criticality changes in the repository with and without FPs

Y. Fukaya:
Optimization of Disposal Method and Scenario to Reduce High Level Waste Volume and Repository Footprint for HTGR

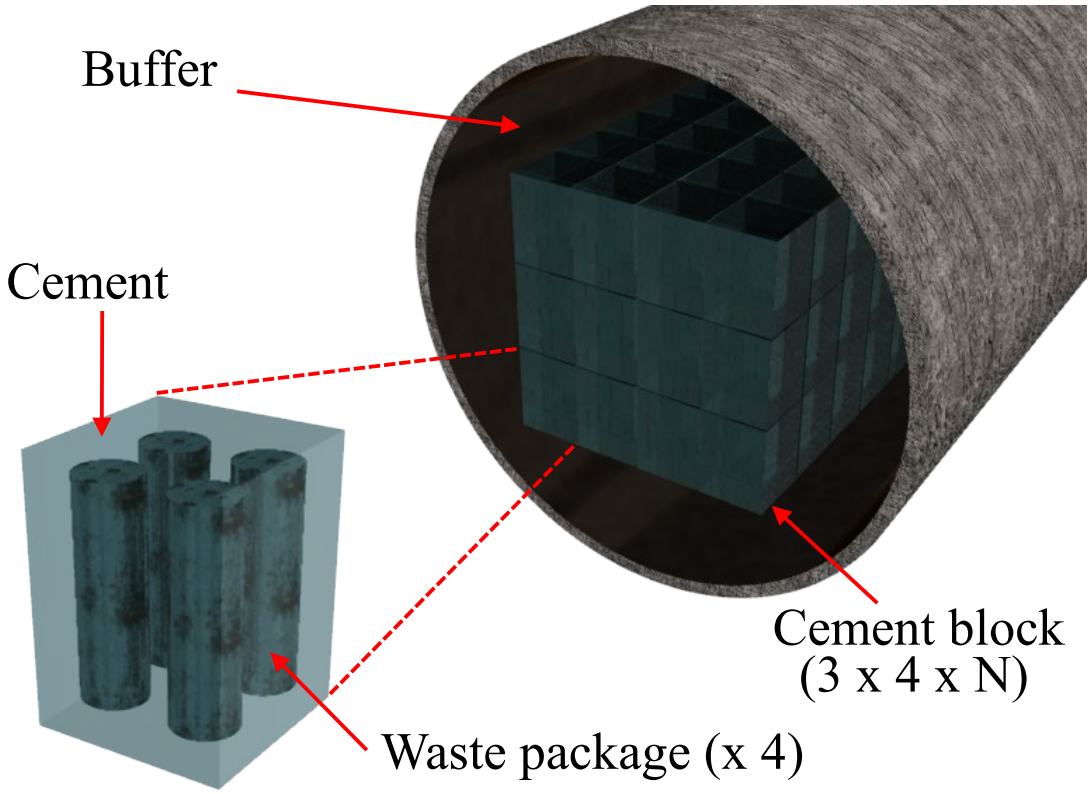

Fig.8 Concept of compact emplacement

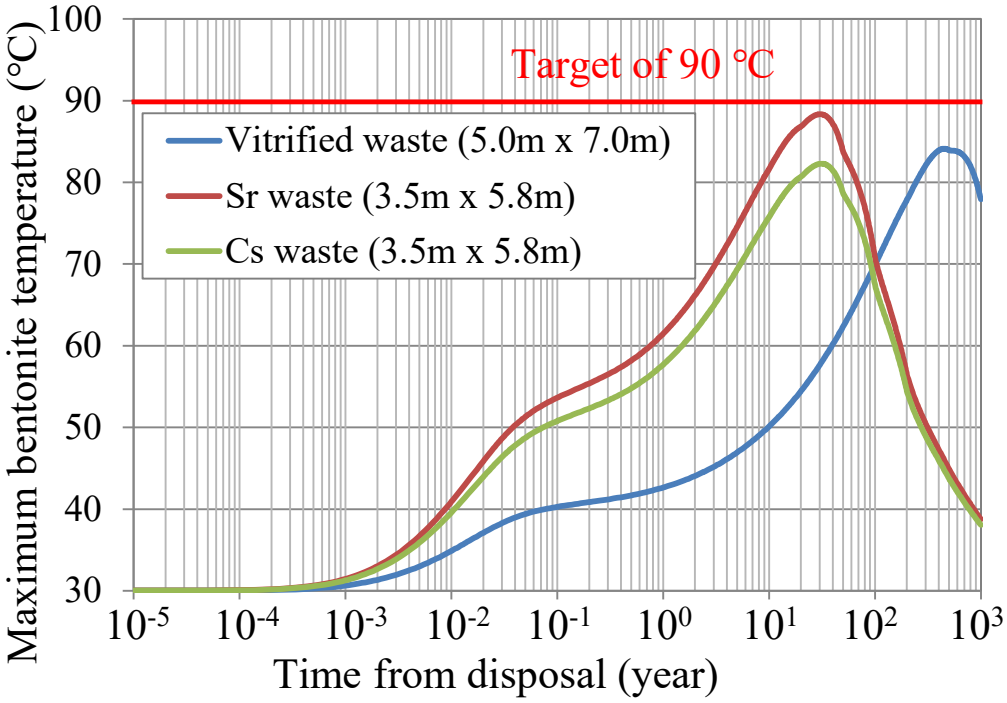

* Values in parentheses give the canister pitch times the drift interval.

Fig.9 Maximum bentonite temperature with partitioning

Y. Fukaya:

Optimization of Disposal Method and Scenario to Reduce High Level Waste Volume and Repository Footprint for HTGR

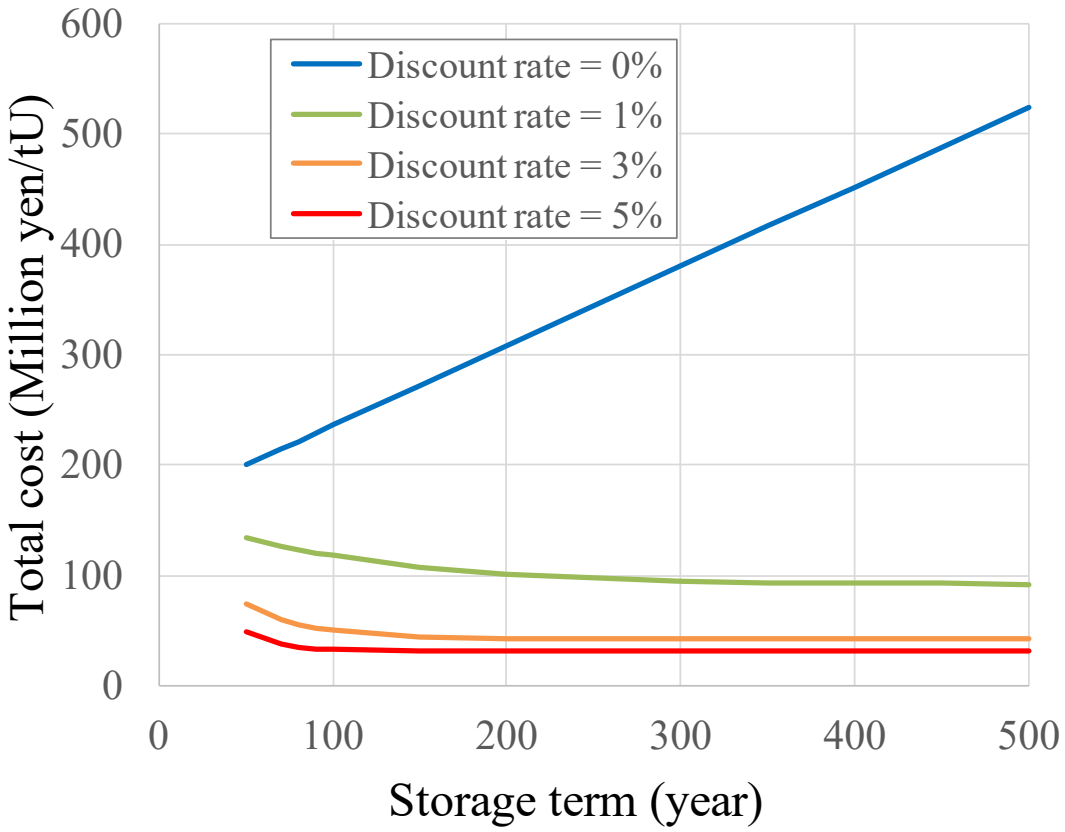

Fig.10 Total back-end costs as functions of storage term at terms discount rates